



# The passivity of titanium—part III: characterization of the anodic oxide film

Bumwook Roh<sup>1</sup> · Digby D. Macdonald<sup>2</sup>

Received: 3 August 2018 / Revised: 21 March 2019 / Accepted: 22 March 2019 / Published online: 17 May 2019  
© Springer-Verlag GmbH Germany, part of Springer Nature 2019

## Abstract

The thickness of the anodic titanium oxide film formed on titanium in 0.5 M H<sub>2</sub>SO<sub>4</sub> at 22 °C was measured by ellipsometry, and the Forouhi interband single-layer model was used to analyze the data. The anodizing constant was determined experimentally to be 2.75 nm/V, which is in good agreement with literature data, and indicates that the anodizing constants for barrier layers of anodic oxide films formed on a wide variety of metals and alloys lie within the range of 2.2–3.0 nm/V. Using a value for the polarizability of the barrier layer/solution interface obtained via electrochemical impedance spectroscopy (EIS) together with the anodizing constant, the electric field is estimated to be a voltage-independent  $1.82 \times 10^6$  V/cm. For the anodic oxide film formed on titanium in 0.5 M H<sub>2</sub>SO<sub>4</sub> solution by galvanostatic polarization, the thickness was maintained to be virtually constant even though the oxygen vacancy concentration (donor density) analyzed by the Mott-Schottky relation varied over a wide range, as a function of the film formation rate (current density), with higher donor densities being found for lower current densities. The increase in the donor density leads to a decrease in the modulus of the impedance.

**Keywords** Titanium · Passive state · Defect structure · Ellipsometry

## Introduction

A number of studies [1–18] of the properties, on the structure, defect type, and thickness of the anodic oxide film grown on titanium over a wide potential interval have been reported over the past years. For example, with regard to the structure of the anodic titanium oxide film, some studies [7, 18] report that the passive titanium oxide film is multi-layered and has an outermost layer of stoichiometric TiO<sub>2</sub> and an inner oxide comprising a mixture of TiO<sub>2</sub>, Ti<sub>2</sub>O<sub>3</sub>, and TiO, or it is highly oxygen deficient (TiO<sub>2-x</sub>). However, Ohtsuka [2] reports that

the single-layer model should be adopted in the study of anodic titanium oxide. One of the most effective, indirect ways of characterizing the structure of an anodic oxide is to analyze the oxide film thickness using ellipsometry, with which we can model the structure of the film in terms of single- or multi-layered model by optimization upon the ellipsometry data [2, 19]. This is the principal reason for using ellipsometry in the present work, in addition to the fact that it is an accurate, quick, and non-destructive method for measuring film thickness [20].

In the present work, potentiostatic and galvanostatic methods were used for growing the anodic titanium oxide film. In order to investigate the semi-conductive properties of the anodic oxide film on titanium and to ascertain the concentration of the point defects, Mott-Schottky analysis was adopted, where the donor or acceptor concentration is obtained from the slope of  $1/C^2$  versus potential, where  $C$  is the interphasial capacitance.

The results of this work are analyzed upon the basis of the point defect model [21–24], which was developed to describe the growth and breakdown of passive films in terms of the generation and annihilation of point defects (metal and oxygen vacancies and metal interstitials) in the barrier layer of a bi-layer passive film.

---

Passivity of titanium, part 1: film growth model diagnostics was published in (2014) *J Solid State Electrochem* 18:1485-1493; part 2: the defect structure of the anodic oxide film was published in (2019) *J Solid State Electrochem* <https://doi.org/10.1007/s10008-019-04254-0>.

✉ Digby D. Macdonald  
macdonald@berkeley.edu

<sup>1</sup> Hyundai Motor Company, Mabuk-Ri, Hwaseong, Gyeonggi-Do, Republic of Korea

<sup>2</sup> Departments of Nuclear Engineering and Materials Science and Engineering, University of California at Berkeley, Berkeley, CA 94720, USA

## Experimental

The working electrode was a flat disc of titanium (Aldrich, 99.99%) of 0.635-cm diameter. One face of the specimen was mechanically polished through 1200-grit emery papers, and then, successively, with 9-, 3-, and 1- $\mu\text{m}$  diamond powders, and then finally rinsed with D.I. water. All electrochemical experiments were carried out in a flat cell (EG&G PARC) at ambient temperature ( $20 \pm 2$  °C). A PTFE O-ring was used to form a seal between the edge of the sample and the cell.

The electrolyte used was an aqueous solution of 0.5 M  $\text{H}_2\text{SO}_4$  prepared from analytical-grade sulfuric acid and deionized-distilled water. The electrolyte was deoxygenated by sparging with pure nitrogen gas (99.99%), before initiating the growth of the passive film. To avoid back diffusion of  $\text{O}_2$ , and to minimize contamination of the solution with oxygen or hydrogen that might be evolved at the counter electrode, a slow nitrogen flow was continued during the experiment. The electrode potential was measured against a saturated calomel electrode (SCE) and the cell contained a platinum counter electrode. All potentials were converted onto the standard hydrogen electrode (SHE) scale.

The anodic oxide films were grown under either potentiostatic or galvanostatic conditions, which were chosen according to the requirements of the experiments. The potentiostatic method was used to grow the oxide film on titanium for at least 8 h, prior to investigating the film thickness and the film structure using ellipsometry. Also, in order to explore the donor density behavior, anodic oxide films were grown galvanostatically at various current densities, ranging from 10 to 100  $\text{mA}/\text{cm}^2$ , until a potential of 20.0  $V_{\text{SHE}}$  was achieved, at which point the sample was maintained potentiostatically for 2 min. The oxide grows quickly if the voltage is increased in the positive direction from the formation voltage, but it thins very slowly if the voltage is displaced in the negative direction, due to the very low rate of dissolution. Accordingly, a film formed at a higher voltage is dimensionally stable under excursions to lower potentials but not under excursions to higher potentials.

A vertical type of ellipsometer (SOPRA, Model: GES 5) was used to measure the anodic oxide film thickness. The ex situ thickness was measured in air by the highly collimated multiple-monochromatic incidence light. The polarizer and compensator were placed in the incidence light path, and the analyzer and detector were placed in the reflected light path.

The impedance was measured at a frequency of 1.0 kHz, from which capacitance data were extracted for Mott-Schottky analysis. A Solartron 1268 potentiostat connected to a Solartron 1250 frequency response analyzer was used for the impedance measurement with a sinusoidal voltage perturbation having a peak-to-peak excitation amplitude of 10 mV superimposed on the desired, constant polarization voltage. During the capacitance measurements, the voltage

was swept in the negative direction from the voltage of 1.74 to 0.24  $V_{\text{SHE}}$  at 75 mV/s in order to maintain the film thickness and defect concentration approximately constant and hence to ensure better confluence between theory and experiment.

## Results and discussion

### Ellipsometry results

The anodic oxide film on titanium comprises  $\text{TiO}_{2-x}$  with the principal defect being the oxygen vacancy, as previously reported [3, 5, 25, 26] and further discussed in part II of this series [27]. The oxide films have colors ranging from yellow to dark blue as the thickness increases, indicating a high optical absorbance, which is typical of a highly defective phase. Notably absent was the white,  $\text{TiO}_2$  stoichiometric phase that normally comprises the outer layer, and this fact is discussed below in association with the ellipsometry analysis.

The anodic titanium oxide film was formed by the potentiostatic method, and the thickness was determined by ellipsometry. Ellipsometry is an optical analysis technique capable of measuring film thickness based on the optical constants (refractive index ( $n$ ) and extinction coefficient ( $k$ )) of the substrate and the film. It is a non-destructive technique and can measure changes in film thickness in the angstrom range if the optical constants are known with great accuracy and if the surface is highly planar at the nanoscale. As noted above, the structure of uni- or multi-layered film is modeled to fit with the ellipsometry data [2, 19], and in the present work, a “simpler-better” rule was followed. Thus, a single-layer model was used to analyze ellipsometry data, which is consistent with the lack of any white, stoichiometric  $\text{TiO}_2$  being detected on the surface. Use of a multi-layer model did not improve the optimization.

Ellipsometry [20] involves the measurement of the change in the state of polarization of light upon reflection from the sample surface. The state of polarization is defined by the phase and amplitude relationships between the two component plane waves, the p wave perpendicular to the reflective surface and s wave parallel to the plane of incidence. In general, reflection causes a change in relative phases of the p and s waves and a change in the ratio of their amplitudes, because the two components travel different path lengths with the p wave being reflected at the metal/film interface and the s wave being reflected at the film/solution interface. The change in relative phase difference between the p and s waves before and after reflection is characterized by  $\cos(\Delta)$ :

$$\cos\Delta = \partial_1 - \partial_2 \quad (1)$$

while the amplitude ratio change before and after reflection is characterized by  $\tan(\Psi)$  in Eq. (2).

$$\tan\Psi = |R^P|/|R^S| \quad (2)$$

When the two waves recombine after reflection, and as a result of having traveled slightly different distances, the light is elliptically polarized (hence, the name “ellipsometry”). Accordingly, an ellipsometric measurement essentially involves the determination of  $\cos(\Delta)$  and  $\tan(\Psi)$ . These two parameters are a function of the complex index of refraction,  $N = n - ik$ , and film thickness,  $d$ . Therefore, if the optical constants are known, the film thickness can be determined. In the present work, in order to determine the complex index of refraction, the interband transition dispersion formula developed by Forouhi and Bloomer [28, 29] was applied. This is a single-layer model based on the quantum theory of absorption. An expression for the imaginary part,  $k$ , of the complex index of refraction is derived as a function of photon energy  $E$ , and then  $n$ , the real part of the complex index of refraction, is determined by using Kramers-Kronig transformation [20].

Spectroscopic ellipsometry, in which the wavelength is scanned, was used in this work. The wavelength range of the experiments was 250 to 800 nm. The ellipsometric measurement resulted in  $\tan(\Psi)$  and  $\cos(\Delta)$  loci as a function of the wavelength of the incident monochromatic light that were in good agreement with the theoretical lines for an anodic titanium oxide film potentiostatically formed at 3.24, 4.24, 5.24, and 7.24  $V_{SHE}$ . Since the film was found to grow coincidentally with the theoretical curve for a single-layer model, the results provide convincing evidence that the use of the single-layer model to describe the thickness and impedance properties of the anodic titanium oxide film is justified.

The measured thickness versus film formation potential is shown in Fig. 1, where the measured oxide film thickness is compared with the experimental data reported by Ohtsuka [2]. From these plots, the anodizing constants for film growth were determined to be 2.75 nm/V from this work and 2.50 nm/V from the work of Ohtsuka [2] within the respective potential ranges. Both of these experimental anodizing constants are in good agreement with literature data reporting that the anodizing constant for barrier layers of anodic oxide films is ubiquitously 2.2–3.0 nm/V [2, 22, 30]. Accordingly, we conclude that the surface exposed to the solution is that of the single-layered, defective barrier oxide. This experimental result of thickness is compared with the calculated anodic oxide film thickness from the PDM with EIS data in future Part IV [31] of this series.

In order to vary the donor density without changing the film thickness, the anodic oxide films were grown galvanostatically at various current densities ranging from 10 to 100 mA/cm<sup>2</sup>, until a potential of 20.0  $V_{SHE}$  was achieved. After attaining that potential, the sample was maintained at that voltage potentiostatically for 2 min. This is an empirically derived method, but it is consistent with the experimental results of Ohtsuka and Otsuki [32]. This method

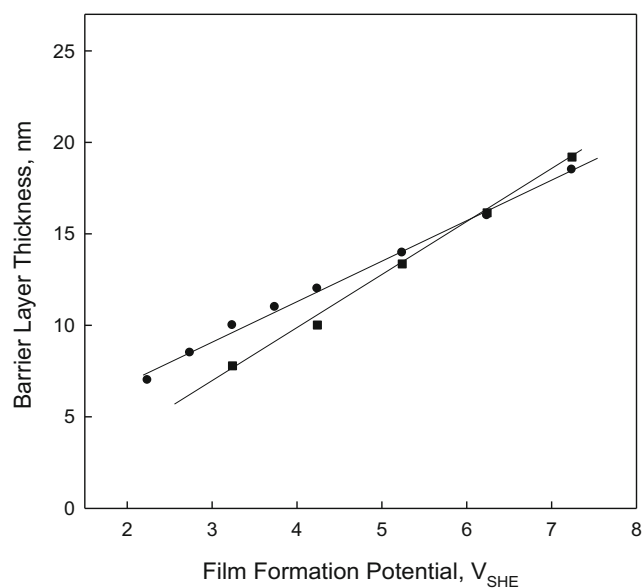
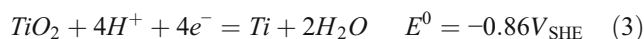


**Fig. 1** Thickness as a function of potential for the anodic oxide film formed on titanium by potentiostatic oxidation, ■ measured in this study in 0.5 M  $H_2SO_4$  solution, ● measured by Ohtsuka [2] in 0.1 M  $H_2SO_4$  solution

was devised to control the oxygen vacancy concentration without changing the film thickness. Specimens prepared this way were used to previously demonstrate [33] that the rate of the oxygen electrode reaction on passive Ti depends upon the surface oxygen vacancy concentration, with the vacancies acting as catalytic species. To our knowledge, this previous work of Roh and Macdonald [33] provides the first demonstration of the catalytic role of surface oxygen vacancies in the oxygen electrode reaction, forming an unequivocal link between the kinetics of this important reaction on an oxide and the defect structure of the substrate. This relationship may be exploited in designing new non-platinum group electrocatalysts. Figure 2 shows the oxide film thickness as a function of current density, measured after growth using the ellipsometer. The thickness decreases slightly with increasing film formation current density, but the thickness is virtually constant within the range of 42–47 nm.

We take the standard potential for the formation of  $TiO_2$  on titanium, as calculated from thermodynamics [34], as



Note that, for a 0.5 M  $H_2SO_4$  solution of pH = 0, this value is virtually the same as the equilibrium potential, which is to be compared with the potential of 20.86  $V_{SHE}$  at which the film was grown. Thus, the thickness of the barrier layer is expected to be  $(20.86 \text{ V}) \times (2.2 \text{ to } 2.5 \text{ nm/V}) = 45.9 \text{ to } 52.2 \text{ nm}$ , which is in good agreement with the  $44.7 \pm 2.0 \text{ nm}$  measured by ellipsometry. This is also strong evidence that the passive film formed on titanium under the conditions employed in this work comprises the barrier layer alone.

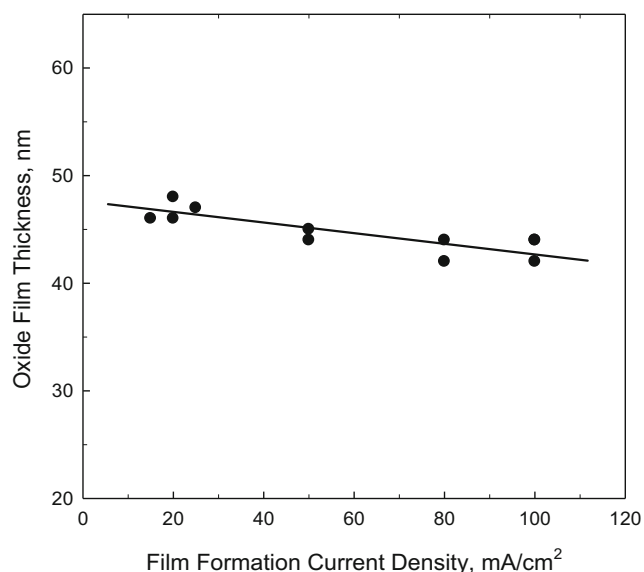


**Fig. 2** Variation of anodic oxide film thickness on titanium formed with various formation current densities, with the final stage of growth being carried out potentiostatically at 20.0 V<sub>SHE</sub>

Accordingly, the outer surface of the passive film is that of the defective barrier layer.

The linear dependence of the film thickness on the formation voltage is in accordance with the predictions of the point defect model [22–25], which yields the following equation for the barrier layer thickness for the case where no change in the oxidation state of the cation in the barrier layer occurs upon ejection at the barrier layer/solution (bl/s) interface or upon dissolution of the film.

$$L_{ss} = \left[ \frac{1-\alpha}{\varepsilon} \right] V + \left[ \frac{2.303n}{\alpha_3 \varepsilon \chi \gamma} - \frac{\beta}{\varepsilon} \right] pH + \frac{1}{\alpha_3 \varepsilon \chi \gamma} \ln \left( \frac{k_3^0}{k_7^0} \right) \quad (4)$$

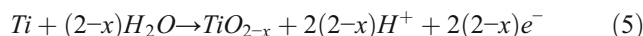
where  $\alpha$ ,  $\beta$ , and  $\varepsilon$  are the polarizability of the bl/s interface (i.e., the dependence of the voltage drop across this interface on the applied voltage); the dependence of the same voltage drop on pH; and the electric field strength in the barrier layer, respectively,  $n$  is the kinetic order of the barrier layer dissolution rate with respect to  $H^+$ ,  $\gamma = F/RT$ ,  $\chi$  is the oxidation state of the cation in the barrier layer,  $k_3^0$  and  $\alpha_3$  are the standard rate constant and transfer coefficient of the film growth reaction at the metal/barrier layer (m/bl) interface, respectively, and  $k_7^0$  is the standard rate constant for the barrier layer dissolution reaction at the bl/s interface. The anodizing constant is  $(\partial L_{ss} / \partial V)_{pH} = (1 - \alpha) / \varepsilon$ .

Figure 1 shows that the steady-state barrier layer thickness varies linearly with formation voltage from which we calculate  $dL_{ss}/dV = 2.75$  nm/V, which is in good agreement with literature data, which indicate that the anodizing constants for barrier layers of anodic oxide films formed on a wide variety of metals and alloys lie within the range of 2.2–3.0 nm/V, as noted previously. From part IV [31] of this series, we find, from

electrochemical impedance spectroscopy (EIS), that  $\alpha = 0.498$ . Thus, from the definition of the anodizing constant, given above, and the value of  $\alpha$ , we find that the electric field strength is  $1.82 \times 10^6$  V/cm. This value is within the range of  $1 \times 10^6$  to  $3 \times 10^6$  V/cm that is normally found for passive metals [22–24].

## EIS and Mott-Schottky analysis results

The growth of thin, anodic oxide layers on titanium at voltages within the range employed in this work (2.1 to 7.2 V<sub>SHE</sub>) is known to take place irreversibly according to the following reaction:



where we write the oxide in a form emphasizing that the barrier layer forms as an oxygen-deficient phase.

As mentioned previously, in order to obtain the donor density (oxygen vacancy concentration), and hence the non-stoichiometry of the passive film, as a function of the formation conditions, the anodic oxide films were grown galvanostatically at different current densities and the oxygen vacancy concentration was analyzed with the Mott-Schottky plots. Mott-Schottky plots [35] of  $C^{-2}$  vs.  $V$  were derived from the capacitance  $C$  obtained from  $C = -1/(\omega Z''')$ , where  $Z'''$  is the imaginary component of the impedance measured at a frequency of 1.0 kHz. However, measurements were also made at 10 kHz and are reported in part II [27]. Little frequency dispersion was found in the measured capacitance, as noted below. In using the Mott-Schottky equation, it is assumed that the capacitance of the double layer ( $C_{dl}$ ) on the solution side of the interface is much larger than the space charge capacitance ( $C_{sc}$ ) of the oxide film, and that these capacitances exist in series. Bondarenko and Ragoisha [8] have used potentiodynamic electrochemical impedance spectroscopy (PDEIS) to measure the space charge capacitance of anodic TiO<sub>2</sub> in 1.0 M H<sub>2</sub>SO<sub>4</sub> at potentials up to 600 mV vs Ag/AgCl/KCl(sat). The value for the space charge capacitance is calculated from their Mott-Schottky plots to be about 5  $\mu\text{F}/\text{cm}^2$ . Because the double layer capacitance is of the order of 20–50  $\mu\text{F}/\text{cm}^2$ , the condition that  $C_{dl} \gg C_{sc}$  is fulfilled and the measured capacitance can be equated to  $C_{sc}$ . Plots of  $C^{-2}$  vs.  $V_{SHE}$  display a positive slope that is characteristic of an n-type semiconductor (see below), and the value of the slope may be used to estimate the donor density. The defect structure of a passive film on titanium is well accounted for in terms of the point defect model (PDM) [21–24], and evidence for this defect assignment can be found elsewhere [3, 36–38].

The space charge capacitance of an n-type semiconductor is given by Mott-Schottky theory [35] as Eq. 6:

$$C^{-2} = \frac{2}{e \varepsilon_0 \varepsilon_r N_D A^2} (V - V_b - kT/e) \quad (6)$$

where  $A$ ,  $\epsilon_0$ ,  $\epsilon_r$ , and  $N_d$  are, respectively, the geometrical surface area, the vacuum permittivity, the dielectric constant of the oxide, and the donor concentration.  $V$  is the applied potential,  $V_{fb}$  is the flat band potential, and  $e$  is the charge of the electron ( $1.6 \times 10^{-19}$  C). The value of the dielectric constant used to calculate the donor density was chosen to be 45 as in the work of Marsh et al. [39] and Kudelka and co-workers [40].

Typical Bode plots of the real and imaginary components of the impedance of passive titanium versus frequency are shown in Fig. 3. The spectra were recorded at a potential of 1.24 V<sub>SHE</sub>, with a sinusoidal voltage amplitude of 10 mV peak-to-peak. In this figure, it is shown that at frequencies higher than ~600 Hz the real part of the impedance displays little dependence on frequency and approaches a constant value. Accordingly, at sufficiently high frequency, the frequency dependence of the impedance is governed by the imaginary component, from which the capacitance was calculated by Mott-Schottky analysis. Thus, Mott-Schottky analysis was performed using the capacitance calculated from the imaginary component measured at a frequency of 1.0 kHz.

Figure 4 shows the Mott-Schottky plot, and the evaluated donor density,  $N_d$ , is plotted in Fig. 5 as a function of the film formation current density. These data show that the donor density decreases with increasing film formation current density, from  $9.15 \times 10^{19} \text{ cm}^{-3}$  at a film formation current density of 10 mA/cm<sup>2</sup> to about  $6.38 \times 10^{18} \text{ cm}^{-3}$  at a current density of 100 mA/cm<sup>2</sup>. This result is in general agreement with the findings of previous studies [32, 41, 42]. The donor concentration measured in this work indicates that the extent of non-stoichiometry,  $x$ , varies from 0.000192 to 0.00171, for formation current

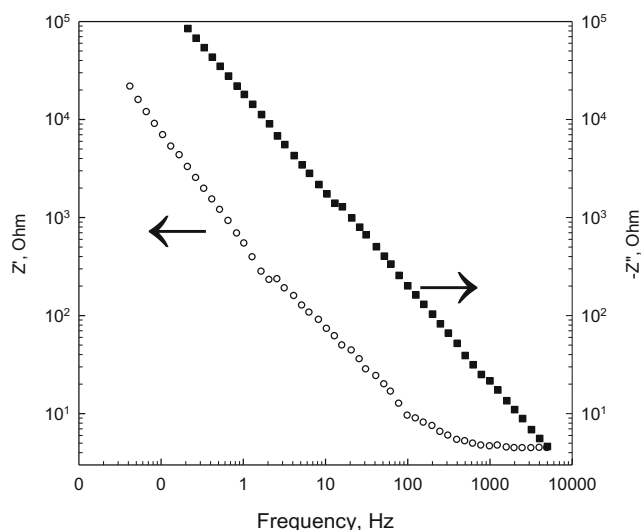


**Fig. 3** Electrochemical impedance spectra for the anodic oxide film formed on titanium at 10 mA/cm<sup>2</sup>, recorded at a potential of 1.24 V<sub>SHE</sub> with alternating voltage amplitude of 10 mV. (○)  $Z'$ , (■)  $Z''$

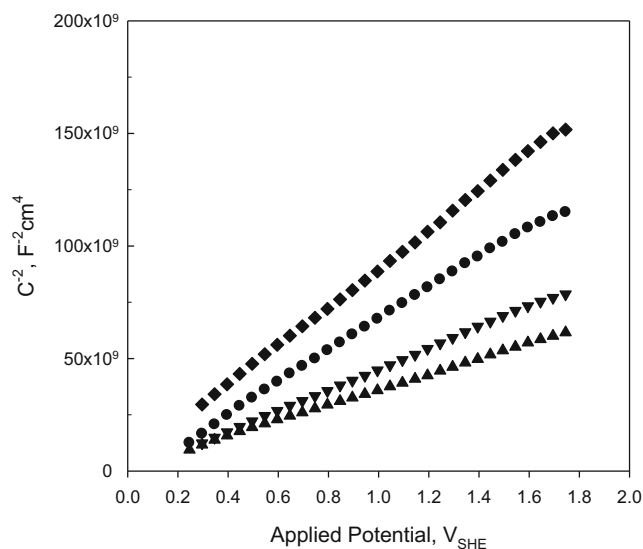


**Fig. 4** Mott-Schottky plots for passive titanium of various defect densities, as measured at a frequency of 1.0 kHz. Film formation current density: (◆) 25 mA/cm<sup>2</sup>, (●) 20 mA/cm<sup>2</sup>, (▼) 15 mA/cm<sup>2</sup>, and (▲) 10 mA/cm<sup>2</sup>

densities of 100 to 10 mA/cm<sup>2</sup>, based upon a tetragonal unit cell having an oxygen sublattice site concentration of  $1.071 \times 10^{23} / \text{cm}^3$  (average of the unit cell volumes of rutile and anatase) and the donor (oxygen vacancy) concentrations given below. This may be compared with oxygen deficiencies (value of  $x$ ) of 0.32 to 0 reported by Triana, Granqvist, and Niklasson [9]. Thus, the anodic oxide on Ti appears to possess a relatively low non-stoichiometry compared with the range that is possible in this material.

Figures 6 and 7 show electrochemical impedance spectra for passive titanium prepared at the various donor

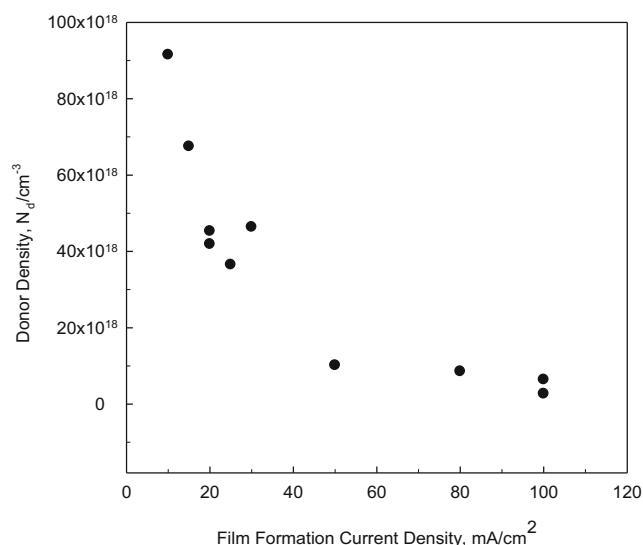


**Fig. 5** Variation of the donor density in the anodic oxide film formed on titanium in 0.5 M H<sub>2</sub>SO<sub>4</sub> solution as a function of formation current density

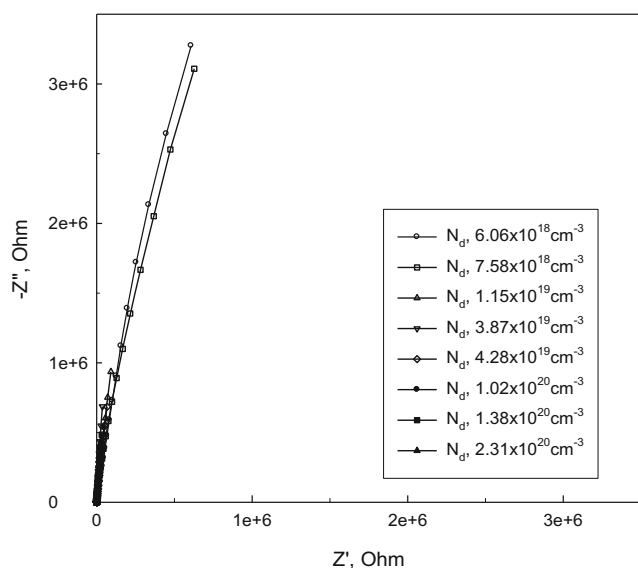


**Fig. 6** Effect of donor (oxygen vacancy) density on the complex-plane impedance spectra for passive titanium measured at a voltage of 1.24  $V_{\text{SHE}}$  in 0.5 M  $\text{H}_2\text{SO}_4$  solution

concentration (and hence formation current densities), as described above. Figure 6 displays typical Nyquist plots obtained under potentiostatic control at 1.24  $V_{\text{SHE}}$  and measured over the frequency range of 0.05 to 5000 Hz. The form of the plots is typical of that observed on valve metals with the loci being almost vertical in the complex plane, because of the dominance of the capacitance. We observe, however, that the modulus of the impedance,  $|Z|$ , is a sensitive function of the donor density, with  $|Z|$  becoming lower as  $N_d$  increases, as shown in Fig. 7. The gradients of the  $\log |Z|$  versus  $\log(f)$  plots in Fig. 7 are almost unity, as expected for an essentially

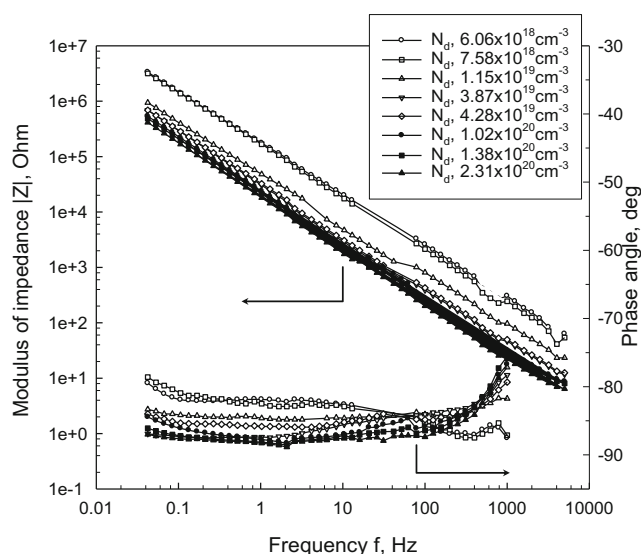


**Fig. 7** Bode plots of the impedance modulus and phase angle as a function of donor (oxygen vacancy) density in the anodic oxide film formed on titanium to a constant thickness of  $44.7 \pm 2$  nm

capacitive interface, and the lack of any tendency for  $|Z|$  to attain a constant value at either limitingly high or low frequency indicates that the film is dominated by this capacitance in its electrical characteristics, as expected, with the capacitance increasing with an increase in the donor concentration. However, it is also evident that the amplitude of the impedance decreases with increasing donor concentration (Fig. 7), which demonstrates that the resistivity decreases in like manner, consistent with the donors facilitating charge transfer through the film. Also, the observed, imaginary component behavior is consistent with the fact that the higher donor density implies a higher space charge capacitance, according to Eq. (6), with the assumption being that the change of the flat band potential does not have much impact upon the relationship between  $C^{-2}$  and  $N_d$ .

## Summary and conclusions

The passive state on titanium in 0.5 M  $\text{H}_2\text{SO}_4$  at ambient temperature (22 °C) has been explored using a combination of ellipsometry, Mott-Schottky analysis, and electrochemical impedance spectroscopy. The findings of this study are as follows:

- The thickness of the anodic titanium oxide film formed was measured by the ellipsometry, and the Forouhi interband uni-layer model was used to analyze the results. The results show that the experimental data from ellipsometry are well described by the calculated theoretical line for a single-layer oxide structure, from which we conclude that a single-layer model for the anodic titanium oxide barrier layer is appropriate.
- The thickness of the single (“barrier”) layer increases linearly with increasing formation voltage, in accordance with the prediction of the point defect model. The thickness data determined in this study are in good agreement with those reported in the literature.
- The passive current density is found to be independent of film formation voltage, which is also in accordance with the prediction of the point defect model for the case of an n-type film where no change in oxidation state occurs upon ejection of a cation at the barrier layer/solution interface or upon dissolution of the film.
- The anodizing constant was determined experimentally to be 2.75 nm/V, which is in good agreement with literature data, indicating that the anodizing constants for barrier layers of anodic oxide films formed on a wide variety of metals and alloys lie within the range of 2.2–3.0 nm/V. Using a value for the polarizability of the barrier layer/solution interface reported elsewhere, the electric field strength was calculated to be  $1.82 \times 10^6$  V/cm. This value

is within the range of  $1 \times 10^6$  to  $4 \times 10^6$  V/cm that is normally found for passive metals.

- For the anodic oxide film formed on titanium in 0.5 M  $\text{H}_2\text{SO}_4$  solution by galvanostatic polarization, the thickness was maintained to be virtually constant even though the oxygen vacancy concentration (donor density) analyzed by the Mott-Schottky relation varied widely as a function of the film formation rate. This experimental result allows the investigation of the kinetics of the oxygen electrode reaction with respect to the oxygen vacancy concentration with the same thickness oxide film.
- Passive titanium displays an almost purely capacitive behavior, which is attributed to the thigh parallel impedance for electron leakage across the barrier layer.
- The donor concentration measured in this work indicates that the extent of non-stoichiometry,  $x$ , varies from 0.000192 to 0.00171, for formation current densities of 100 to 10 mA/cm<sup>2</sup>, based upon a tetragonal unit cell having an oxygen sublattice site concentration of  $1.071 \times 10^{23}/\text{cm}^3$  (average of the unit cell volumes of rutile and anatase) and the donor (oxygen vacancy) concentrations given below.

**Acknowledgments** Investigator no. 2 gratefully acknowledges the partial support of this work by FUTURE (Fundamental Understanding of Transport Under Reactor Extremes), an Energy Frontier Research Center funded by the U.S. Department of Energy (DOE), Office of Science, Basic Energy Sciences (BES).

**Funding information** The study was financially supported by the US Department of Energy through Grant No. DE-FG02-01ER15238 and by the Hyundai Motor Company.

## References

1. Henrich VE, Cox PA (1994) The surface science of metal oxides. Cambridge University Press, Cambridge, UK
2. Ohtsuka T, Masudo M, Sato N (1985) Ellipsometric Study of anodic oxide films on titanium in hydrochloric acid, sulfuric acid, and phosphate solution. *J Electrochem Soc* 132(4):787–792
3. Ellerbrock D (1998) Defect characterization of titanium passive films, Ph. D. Dissertation. Penn State Univ, University Park, PA
4. Diebold U (2003) The surface science of titanium dioxide. *Surf Sci Rep* 48(5-8):53–229
5. Kofstad P (1972) Nonstoichiometry, diffusion, and electrical conductivity in binary metal oxides. Wiley, New York
6. Arsov LD, Kormann C, Plieth W (1991) In Situ Raman Spectra of Anodically Formed Titanium Dioxide Layers in Solutions of  $\text{H}_2\text{SO}_4$ , KOH, and  $\text{HNO}_3$ . *J Electrochem Soc* 138(10):2964–2970
7. Zhu Y-C (1994) Electrochemical and surface analysis of anodic oxide film on titanium and stochastic analysis of pit generation processes on anodized titanium, Ph. D. Dissertation. Osaka University, Osaka, Japan
8. Bondarenko AS, Ragoisha AG (2005) Variable Mott-Schottky plots acquisition by potentiodynamic electrochemical impedance spectroscopy. *J Solid State Electrochem* 9(12):845–849
9. Triana CA, Granqvist CG, Niklasson GA (2016) Optical absorption and small-polaron hopping in oxygen deficient and lithium-ion-intercalated amorphous titanium oxide films. *J Appl Phys* 119(1):015701
10. B-W. Roh,(2007) “Defect properties of anodic oxide films on titanium and impact of oxygen vacancy on oxygen electrode reactions.”, Ph.D. Dissertation, Penn. State University
11. Di Quarto F, Di Franco F, Miraghaei S, Santamaria M, La Mantia F (2017) The amorphous semiconductor Schottky barrier approach to study the electronic properties of anodic films on Ti. *J Electrochem Soc* 164(9):C516–C525
12. Ihara T, Miyoshia M, Iriyamab Y, Matsumoto O, Sugihara S (2003) Visible-light-active titanium oxide photocatalyst realized by an oxygen-deficient structure and by nitrogen doping. *Appl Catal B Environ* 42(4):403–409
13. Shin J, Joo J, Samuelis D, Maier J (2012) Oxygen-deficient  $\text{TiO}_2-\delta$  nanoparticles via hydrogen reduction for high rate capability lithium batteries. *Chem Mater* 24(3):543–551
14. Tang H, Prasad K, Sanjinès R, Schmid PE, Lévy F (1994) Electrical and optical properties of  $\text{TiO}_2$  anatase thin films. *J Appl Phys* 75(4):2042–2047
15. Lee H-Y, Clark SJ, Robertson J (2011) First-principles study of oxygen deficiency in rutile titanium dioxide. *Mater Res Soc Symp Proc* 1352
16. Feng X, Wang P, Qian JJ, Wang C, Ao Y (2018) Oxygen vacancies and phosphorus codoped black titania coated carbon nanotube composite photocatalyst with efficient photocatalytic performance for the degradation of acetaminophen under visible light irradiation. *Chem Eng J* 352:947–956
17. Pelaez M, Nolan NT, Pillai SC, Seery MK, Falaras P, Kontos AG, Dunlop PSM, Hamilton JWJ, Byrne J, O’Shea K, Entezari MH, Dionysiou DD (2012) A review on the visible light active titanium dioxide photocatalysts for environmental applications. *Appl Catal B Environ* 125:331–349
18. El-Basouny MS, Mazhar AA (1982) Electrochemical behavior of passive layers on titanium. *Corrosion* 38(5):237–240
19. Sun L, Hou P (2004) Spectroscopic ellipsometry study on e-beam deposited titanium dioxide films. *Thin Solid Films* 455-456:525–529
20. Tompkins HG (1993) A user’s guide to ellipsometry. Academic Press, Boston
21. Macdonald DD (1992) The point defect model for the passive state. *J Electrochem Soc* 139(12):3434–3449
22. Macdonald DD, Engelhardt GR (2010) The point defect model for bi-layer passive films. *ECS Trans* 28(24):123–144
23. Macdonald DD (2011). (Invited Review) The history of the point defect model for the passive state: a brief review of film growth aspects. *Electrochim Acta* 56(4):1761–1772
24. Macdonald DD (2012) The passive state in our reactive metals-based civilization. *Arab J Sci Eng* 37(5):1143–1185
25. Balachandran U, Eror NG (1988) Electrical conductivity in non-stoichiometric titanium dioxide at elevated temperatures. *J Mater Sci* 23(8):2676–2682
26. Millot F, Blanchin M-G, Tetot R, Marucco J-F, Poumellec B, Picard C, Touzelin B (1987) High temperature nonstoichiometric rutile  $\text{TiO}_2-x$ . *Progress Solid State Chem* 17(4):263–293
27. B.-W. Roh (2019) Passivity of titanium. Part II, The defect structure of the anodic oxide film. *J Solid State Electrochem* (in press)
28. Forouhi AR, Bloomer I (1986) Optical dispersion relations for amorphous semiconductors and amorphous dielectrics. *Phys Rev B* 34(10):7018–7026
29. Forouhi AR, Bloomer I (1988) Optical properties of crystalline semiconductors and dielectrics. *Phys Rev B* 38(3):1865–1874
30. Kozlowski M, Smyrl WH, Atanasoska L, Atanasoski R (1989) Local film thickness and photoresponse of thin anodic  $\text{TiO}_2$  films on polycrystalline titanium. *Electrochim Acta* 34(12):1763–1768

31. B.-W. Roh,(2019) “Passivity of titanium. Part IV, impedance behavior considering only oxygen deficiency”, This Journal, to be submitted
32. Ohtsuka T, Otsuki T (1998) The influence of the growth rate on the semiconductive properties of titanium anodic oxide films. *Corrosion Sci* 40(6):951–958
33. Roh B-W, Macdonald DD (2007) Effect of oxygen vacancies in anodic titanium oxide films on the kinetics of the oxygen electrode reaction. *Russ J Electrochem* 43(2):125–135
34. James WJ, Straumanis ME (1976) *Encyclopedia of electrochemistry of the elements*. Marcel Dekker, New York
35. S. Roy Morrison,(1980) *Electrochemistry at semiconductor and oxidized metal electrodes*. Springer
36. Kim C-H, Pyun S-I, Lee E-J (1991) Donor distribution over anodically passivating crystalline and amorphous TiO<sub>2</sub> films. *Mater Lett* 10:387–391
37. Houlihan JF, Mulay LN (1974) Electronic properties and defect structure of Ti407: correlation of magnetic susceptibility, electrical conductivity, and structural parameters via EPR spectroscopy. *Phys Status Solidi B* 61(2):647–657
38. Leitner K, Schultze JW, Stimming U (1986) Photoelectrochemical investigations of passive films on titanium electrodes. *J Electrochem Soc* 133(8):1561–1568
39. Marsh J, Gorse D (1998) A photoelectrochemical and ac impedance study of anodic titanium oxide films. *Electrochim Acta* 43(7):659–670
40. Kudelka S, Michaelis A, Schultze JW (1995) Electrochemical characterisation of oxide layers on single grains of a polycrystalline Ti-sample. *Ber Bunsenges Phys Chem* 99(8):1020–1027
41. Torresi RM, Camara OR, Pauli CPD, Giordano MC (1987) Hydrogen evolution reaction on anodic titanium oxide films. *Electrochim Acta* 32(9):1291–1301
42. Blackwood DJ, Peter LM (1989) The influence of growth rate on the properties of anodic oxide films on titanium. *Electrochim Acta* 34(11):1505–1511

**Publisher's note** Springer Nature remains neutral with regard to jurisdictional claims in published maps and institutional affiliations.